The American Journal of Human Genetics, Volume *92*

Supplemental Data

Mutations in *ANTXR1* Cause GAPO Syndrome

Viktor Stránecký, Alexander Hoischen, Hana Hartmannová, Maha S. Zaki, Amit Chaudhary, Enrique Zudaire, Lenka Nosková, Veronika Barešová, Anna Přistoupilová, Kateřina Hodaňová, Jana Sovová, Helena Hůlková, Lenka Piherová, Jayne Y. Hehir-Kwa, Deepthi de Silva, Manouri P. Senanayake, Sameh Farrag, Jiří Zeman, Pavel Martásek, Alice Baxová, Hanan H. Afifi, Brad St. Croix, Han G. Brunner, Samia Temtamy, and Stanislav Kmoch

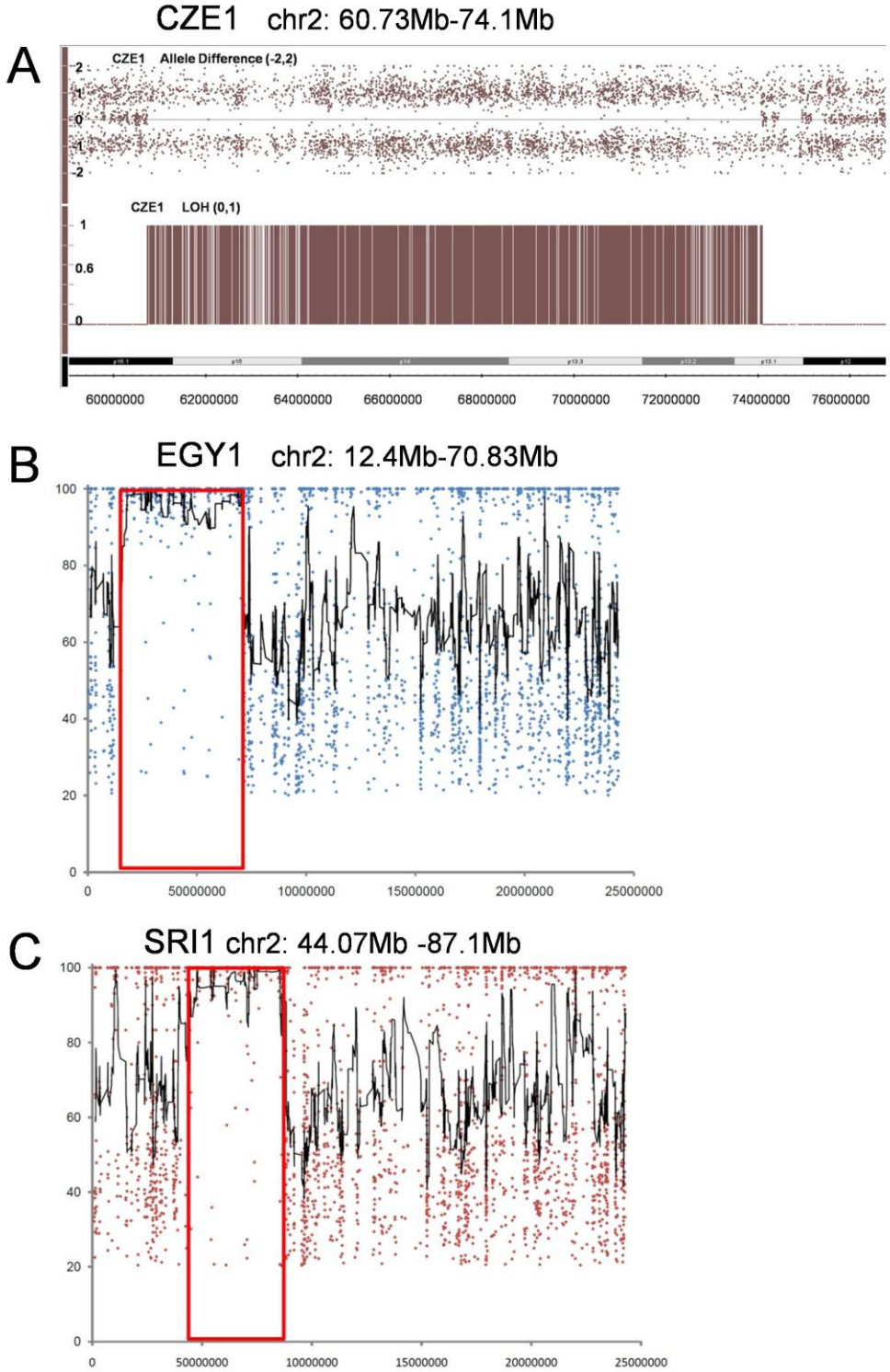

Figure S1. Autozygous Regions on Chromosome 2 Identified in GAPO Cases from families CZE1, EGY1, and SRI1

(A) Genotyping of the case CZE1, (II-1). DNA sample was genotyped using an Affymetrix GeneChip Mapping 6.0 Array (Affymetrix, Santa Clara, CA) at the microarray core facility of the Institute of Molecular Genetics in Prague according to the manufacturer's protocol. Raw feature intensities were extracted from the Affymetrix GeneChip Scanner 3000 7G images using the GeneChip Command Console Software 2.1. Individual SNP calls were generated using Affymetrix Genotyping Console Software 4.1. Copy number changes were identified in Affymetrix Genotyping Console Software (GTC version 4.1). Data from both SNP and copy number probes were used to identify copy number aberrations compared to built-in reference.

Only regions larger than 10 Kb containing at least 5 probes were reported. Extended homozygosity regions (ROHs) were identified in Affymetrix Genotyping Console Software version 4.1 using the algorithm comparing values from the user's sample set and SNP-specific distributions derived from a reference set of two hundred ethnically diverse individuals. Only regions larger than 3 Mb were reported. The minimal size of candidate homozygote regions was set empirically to effectively detect ROH in Affymetrix 6.0 data and to filter out ROHs most commonly found in population data. This approach should identify all "true and unique" ROHs in investigated individuals. It does not account for the degree of consanguinity. In consanguineous individuals the ROH regions are proportionally much larger [1; 2]. (Upper line) shows presence of homozygous (values 1 and -1) and heterozygous genotypes (value 0) within the indicated genomic region on chromosome 2 (x-axis). (Lower line) shows likelihood that a SNP is in „region of heterozygosity state" (ROH) state (value 1, dark line, indicates a significant (strong) likelihood of ROH).

(B and C) Autozygous regions identified by exome sequencing in cases EGY1, (V-3) and SRI1, (IIII-1). Individual dots represent non reference variants; x-axis defines genomic position of the variant, y-axis shows percentage of non reference reads from total reads covering the variant position. Black line shows a moving average of 20 consequent percentage values. Autozygous regions are highlighted by red boxes.

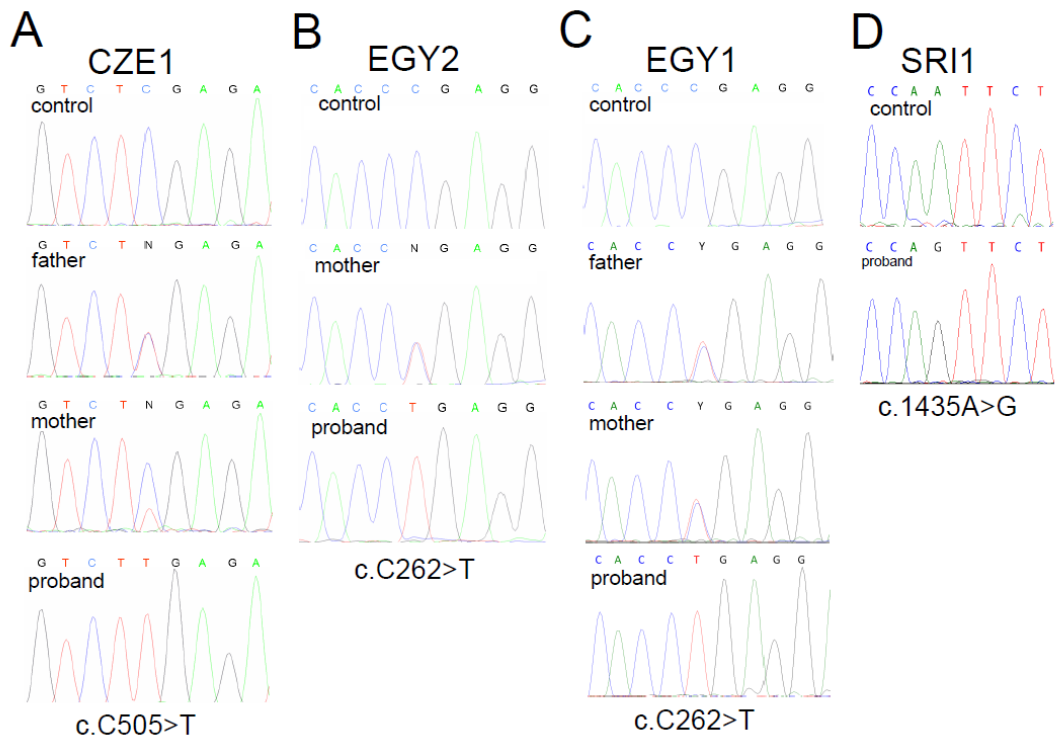

Figure S2. Identification and Analysis of *ANTXR1* Mutation

All of the exons with their corresponding exon-intron boundaries of the *ANTXR1* gene, were PCR amplified from genomic DNA of the probands and sequenced using a version 3.1 Dye Terminator cycle sequencing kit (Applied Biosystems, Foster City, CA) and electrophoresis on an ABI 3500XL Avant Genetic Analyzer (Applied Biosystems). Data were analyzed using Sequencing Analysis software. Segregation of the candidate mutations were assessed either by direct sequencing or restriction enzyme based analysis of the of the corresponding PCR amplified genomic DNA fragments. BsaJI and XhoI restriction enzymes (Fermentas, Vilnius, LT) were used for detection of (c.262C >T; p.Arg88*) and (c.505C >T; p.Arg169*) mutations, respectively. All primers were obtained from Generi Biotech (Hradec Kralove, Czech Republic) and their sequences are provided in Table S3.

(A) Chromatograms of *ANTXR1* genomic DNA sequences showing identified mutations in the Czech family. (Upper panel) Sequence of the unaffected individual, (middle panels) sequences showing heterozygous mutation c.505C>T in the father and mother, and (lower panel) sequence showing homozygous mutation c.505C>T in the proband II-1.

(B) Chromatograms of *ANTXR1* genomic DNA sequences showing identified mutations in the Egyptian family EGY2. (Upper panel) Sequence of the unaffected individual, (middle panels) sequences showing heterozygous mutation c.262C>T in the mother, and (lower panel) sequence showing homozygous mutation c.262C>T in the proband VI-4.

(C) Chromatograms of *ANTXR1* genomic DNA sequences showing identified mutations in the Egyptian family EGY1. (Upper panel) Sequence of the unaffected individual, (middle panels) sequences showing heterozygous mutation c.262C>T in the father and mother, and (lower panel) sequence showing homozygous mutation c.262C>T in the proband V-3.

(D) Chromatograms of *ANTXR1* genomic DNA sequences showing identified mutation in the family SRI1. (Upper panel) Sequence of the unaffected individual, and (lower panel) sequence showing homozygous mutation c.1435-12A>G in the proband III-1.

A

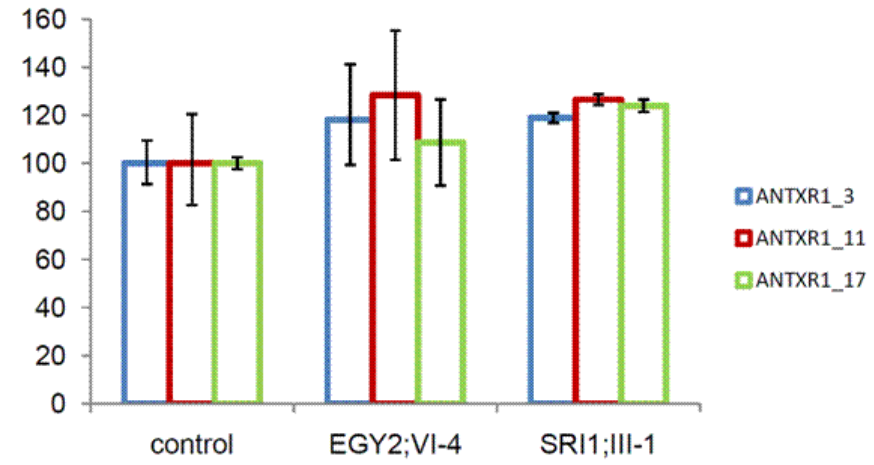

B

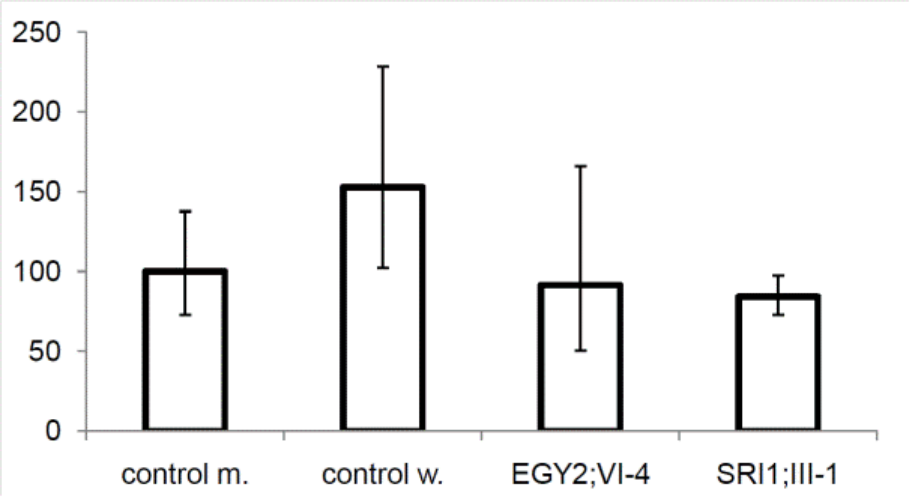

Figure S3. Quantitative PCR Analysis of Genomic DNA

Quantitative PCR was carried out on a StepOne Plus Real Time System (Applied Biosystems). The reactions were carried out in a 96-well plate in a 20-µl reaction volume containing 10 µl of 2×Maxima SYBR Green qPCR Master Mix (Thermo Scientific); 0.2 µM of forward and reverse primer and 20ng of gDNA. The thermal profile for all SYBR Green PCRs was 95°C for 2 min, followed by 45 cycles of 95°C for 10 s, 53°C for 10 s and 72°C for 30 s. Each sample was analyzed three times in three replicates. Data were analyzed by StepOne Software v 2.0. The comparative Ct (ΔΔ Ct) method was used to normalize target genomic fragments.

(A) Amounts of *ANTXR1* exon 3 and mutation harboring exons 11 and 17 relative to exon 12 of autosomal *JUP* in control and indicated cases.

(B) Amounts of the X-linked *FHL1* exon 3 relative to the *ANTXR1* exon 3 in control male (m.), control female (f.) and indicated cases. The means ± SD of three experiments performed in triplicates are shown.

Figure S4. In Silico Splice-Site Prediction for the c.1435-12A>G Mutation in Proband III-1 from Family SRI1

(A) The Alamut (San Diego, CA, U.S.A.) splicing window was used to predict possible effects of the non-coding c.1435-12A>G *ANTXR1* mutation on RNA splicing. This comprises the in silico prediction of the programs SpliceSiteFinder, MaxEntScan, NNSPLICE, GeneSplicer and Human Splicing Finder. All programs (listed on the left) predicted that the A>G nucleotide change creates a novel strong splice acceptor site, that will be preferentially used compared to the original splice acceptor.

(B) The ESE finder software predicts a difference in the binding of the spliceosome induced by the nucleotide change and suggests creation of a new splice acceptor site located 11 bases upstream from the last exon of *ANTXR1*. This novel site is very likely used in patient SRI1,III-1 and hypothetically results in an insertion of 11 additional nucleotides into *ANTXR1* mRNA

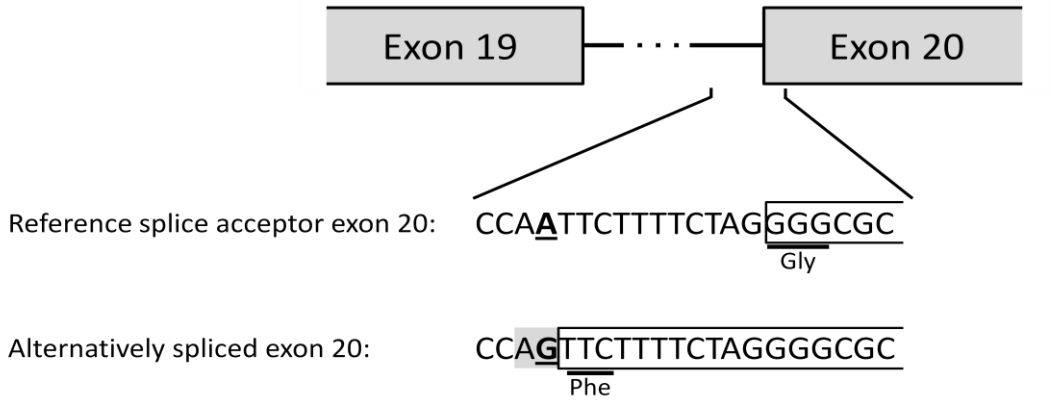

Figure S5. Predicted Effect of the c.1435-12A>G Mutation on *ANTXR1* mRNA Splicing and ANTXR1 Biosynthesis

The homozygous substitution c.1435-12A>G identified in proband III-1 from family SRI1 is predicted to create a new splice acceptor for the last exon of *ANTXR1* (grey boxed AG), resulting in an alternatively spliced last exon that is out of frame. The mutant transcript is predicted to encode for proteosynthesis of a truncated ANTXR1 containing 118 unique amino acids on its C-terminus, p.Gly479Phefs*119.

Chromosome	Start position	SNP id	V-3 EGY1	VI-6 EGY2	Gene name
chr2	69201894	rs4417751	T/T	T/T	*GKN1*
chr2	69204964	n.e.	A/A	C/C	*GKN1*
chr2	69271911	c.262C>T	T/T	T/T	*ANTXR1*
chr2	69300274	rs113138542	T/T	C/C	*ANTXR1*
chr2	69317925	rs4854546	A/A	missing	*ANTXR1*
chr2	69330118	rs6710260	G/G	G/G	*ANTXR1*
chr2	69420591	rs62134900	A/A	T/T	*ANTXR1*
chr2	69472419	rs72903177	T/T	C/C	*ANTXR1*
chr2	69472633	rs72903178	G/G	C/C	*ANTXR1*

Figure S6. Autozygous Haplotypes across the *ANTXR1* Genomic Region Obtained by Exome Sequencing in Case V-3 from Family EGY1 and Sanger Sequencing in Case VI-6 from Family EGY2

Colored boxes show non- concordant genotypes between probands V-3 and VI-6 from families EGY1 and EGY2, respectively. Hypothetical haploinsufficiency around the c.262C>T (p.Arg88*) mutation in *ANTXR*1was excluded in VI-6 by using quantitative PCR of the corresponding genomic fragment (Figure S3). All coordinates refer to hg19; n.e. – non existing; missing – the position was not analyzed.

Table S1. Sequence Variants Revealed by Exome Sequencing in Probands

Individual	CZE1, II-1	EGY1, V-3	SRI1, III-1
Exome Sequencing Statistics			
Total Gb of sequence	6.2	6.1	6.3
Median coverage	-	72.7	72.2
Average coverage	16.1	92.4	93.7
Variant Statistics			
Total number of coding and splice site (SA20nt, SD8nt) variants and indels	15325	19969*	19861*
Number of non-synonymous, splice-site variants and indels	8195	11140	11137
Variants not present in internal exome database nor in dbSNP	560	242**	312**
Novel variants and variants with allele frequency < 0.1 % in EVS database	121	NA	NA
Heterozygous variants	118	227	284
Homozygous variants (≥80% variation)	3 (*ANTXR1*,*ZRSR2*, *DRP2*)	15	28
Homozygous variants located in ROH regions	1 (*ANTXR1*)	NA	NA
Genes with homozygous variants in both individuals	NA	1 (*ANTXR1*)	1 (*ANTXR1*)
Homozygous variants located in overlapping ROH region on chromosome 2	**1 (*ANTXR1*)**	**1 (*ANTXR1*)**	**1 (*ANTXR1*)**
Genes with possible compound heterozygous variants	0	9 (*DIAPH3*, *DNAH17*, *EVC2*, *KAT2A*, *MIR320A*, *NEB*, *PEG3*, *RAB24*, *TTN*)	7 (*ZNF679*, *TTN*, *TDR9*, *RNF213*, *MYOF*, *AGXT2L2*, *ACSBG2*)

*at least 5 variant reads, at least 20% variation; ** filtered against dbSNP134, and Nijmegen in-house database consisting of 1154 exomes

Table S2. Private or Rare Homozygous Variants Identified by Exome Sequencing in Probands with GAPO Syndrome

Chromosome	Position	Reference	Observed	Gene	Accession	cDNA Nucleotide Change	Amino Acid Change	SIFT	PolyPhen-2
					CZE1				
2	**69302734**	**C**	**T**	***ANTXR1***	**NM_018153**	**c.505C>T**	**p.(R169*)**	**1**	**0.73**
X	15841060	A	G	*ZRSR2*	NM_005089	c. 1144A>G	p.(N382D)	0.63	0
X	100486731	G	A	*DRP2*	NM_001939	c.95G>A	p.(R32Q)	0.03	0.08
					EGY1				
1	48708279	C	T	*SLC5A9*	NM_001135181	c.1903C>T	p.(Q635*)	NA	NA
1	53730071	T	C	*LRP8*	NM_004631	c.1428-3A>G	p.(?)	NA	NA
2	39213197	G	A	*SOS1*	NM_005633	c.3770C>T	p.(T1257I)	0.08	0.180
2	27456285	C	T	*CAD*	NM_004341	c.3097C>T	p.(R1033W)	0.00	0.999
2	**69271911**	**C**	**T**	***ANTXR1***	**NM_032208**	**c.262C>T**	**p.(R88*)**	**NA**	**NA**
3	112993378	G	C	*BOC*	NM_033254	c.1391G>C	p.(G464A)	0.69	0.000
3	113286517	T	C	*SIDT1*	NM_017699	c.475T>C	p.(Y159H)	0.00	0.999
3	52413972	C	T	*DNAH1*	NM_015512	c.7429C>T	p.(R2477W)	0.03	NA
5	141248861	C	T	*PCDH1*	NM_032420	c.176G>A	p.(R59Q)	0.26	0.079
8	145741246	C	A	*RECQL4*	NM_004260	c.1160G>A	p.(G387V)	NA	NA
12	83290338	T	A	*TMTC2*	NM_152588	c.1396T>A	p.(Y466N)	0.24	0.012
12	48137331	T	C	*RAPGEF3*	NM_001098531	c.1807A>G	p.(K603E)	0.60	0.993
15	71128690	C	T	*LARP6*	NM_018357	c.355G>A	p.(V119M)	0.00	1.000
X	20153979	A	C	*EIF1AX*	NM_001412	c.101-20T>G	p.(?)	NA	NA
X	151814027	G	A	*GABRQ*	NM_018558	c.278G>A	p.(S93N)	0.00	0.010
					SRI1				
1	79095563	C	G	*IFI44L*	NM_006820	c.686C>G	p.(A229G)	0.12	0.974
2	47202157	G	T	*TTC7A*	NM_020458	c.563G>T	p.(R188L)	0.03	1.000
2	55467328	T	C	*MTIF2*	NM_001005369	c.1706-17A>G	p.(?)	NA	NA
2	61433921	G	C	*USP34*	NM_014709	c.9020C>G	p.(S3007C)	0.01	0.838
2	68772333	A	G	*APLF*	NM_173545	c.1175A>G	p.(H392R)	0.00	0.999
2	**69472345**	**A**	**G**	***ANTXR1***	**NM_032208**	**c.1435-12A>G**	**p.(G479Ffs*119)**[#]	**NA**	**NA**
2	73676617	C	G	*ALMS1*	NM_015120	c.2960G>C	p.(T987S)	0.00	0.999
2	87085549	G	T	*CD8B*	NM_172102	c.44-10C>A	p.(?)	NA	NA
2	53927538	A	G	*ASB3*	NM_001164165	c.1222T>C	p.(S408P)	0.03	0.658
2	55056583	T	G	*EML6*	NM_001039753	c.816T>G	p.(I272M)	0.07	0.997
4	951715	T	C	*TMEM175*	NM_032326	c.946T>C	p.(S316P)	0.00	1.000
4	114899966	G	T	*ARSJ*	NM_024590	c.25C>A	p.(H9N)	0.39	0.001
4	1834464	G	A	*LETM1*	NM_012318	c.1080+7C>T	p.(?)	NA	NA
4	144917458	C	T	*GYPB*	NM_002100	c.271-1G>A	p.(?)	NA	NA
8	17447157	A	G	*PDGFRL*	NM_006207	c.236A>G	p.(K79R)	0.25	0.016
8	42042616	G	T	*PLAT*	NM_000930	c.614C>A	p.(T205N)	0.04	0.828
10	118236315	G	A	*PNLIPRP3*	NM_001011709	c.1324G>A	p.(G442R)	0.16	0.985
10	50190609	G	A	*WDFY4*	NM_020945	c.9544G>A	p.(A3182T)	0.09	0.003
11	74554471	C	T	*XRRA1*	NM_182969	c.2153G>A	p.(R718Q)	1.00	0.008

11	75160580	C	T	*GDPD5*	NM_030792	c.550G>A	p.(A184T)	0.22	0.219
11	101762300	C	G	*ANGPTL5*	NM_178127	c.877G>C	p.(D293H)	0.01	0.808
17	56283513	C	T	*MKS1*	NM_017777	c.1607G>A	p.(R536Q)	0.00	1.000
19	42383347	C	T	*CD79A*	NM_001783	c.367C>T	p.(L123F)	0.00	1.000
X	36162799	G	A	*CXorf59*	NM_173695	c.1382G>A	p.(R461K)	0.56	0.880
X	39921666	C	T	*BCOR*	NM_017745	c.4072-20G>A	p.(?)	NA	NA
X	131762517	G	A	*HS6ST2*	NM_001077188	c.1552G>A	p.(R558C)	0.50	0.883
X	134713730	G	A	*DDX26B*	NM_182540	2026G>A	p.(D676N)	0.28	0.003
X	152959970	C	T	*SLC6A8*	NM_001142805	c.1466-18C>T	p.(?)	NA	NA

All coordinates refer to hg19; [#] based on prediction of Alamut splicing window *in silico* prediction; NA - not analyzed.

Table S3. Oligonucleotides Used in This Study

Primers for PCR Amplification of Coding Regions of *ANTXR1*

Name	Sequence 5´- 3´	Genomic Position
ANTXR1_1F	GAATAAAGGACCCGCGAGGAA	2:69240523-69240543
ANTXR1_1R	CAACAAAGGCGCAGCACTCCG	2:69240924-69240944
ANTXR1_2F	GAACCCTAACAGAAAGTTGAA	2:69266997-69267017
ANTXR1_2R	GAGAAGGGAGAATGCTAAATA	2:69267479-69267499
ANTXR1_3F	TTCAGTTCTGGCAGCCGTGAT	2:69271766-69271786
ANTXR1_3R	ACCCATGTGCCCATACGTAAG	2:69272082-69272102
ANTXR1_45F	TCCTGTGTTATGGTTGACCCT	2:69297598-69297618
ANTXR1_45R	GAATTTGACCCAATACATGCC	2:69299081-69299101
ANTXR1_6F	ATTGACTTTGGGTGGTTGAAC	2:69300047-69300067
ANTXR1_6R	AAAGGGGAAAACATTTACCAT	2:69300420-69300440
ANTXR1_7F	AAGCCCTTCATCAAGACTCTA	2:69302482-69302502
ANTXR1_7R	CTTTTGACATCCTGGCAATTT	2:69303027-69303047
ANTXR1_8F	TAAAAGCTGGAGCCAACCCTT	2:69304321-69304341
ANTXR1_8R	CCACAGTCTGCCCAGTTAGGA	2:69304889-69304909
ANTXR1_9F	CCCAACAGCATCTAGCACAAT	2:69317791-69317811
ANTXR1_9R	TGCTTGGATTACAGGCATAAG	2:69318305-69318325
ANTXR1_10F	GAAGGTGTTCTGCGTTAGGAG	2:69329702-69329722
ANTXR1_10R	TGACTGGAACCACTGTAAGGG	2:69330221-69330241
ANTXR1_11F	TTTCTGTCCTTGCGATAGTTT	2:69349983-69350003
ANTXR1_11R	GCTCCACTTTCTCTAGATGCT	2:69350294-69350314
ANTXR1_12F	CTTTAAAGGAGGATGGGCTAT	2:69351497-69351517
ANTXR1_12R	GTACAGCACACCCCAATCCAG	2:69351934-69351954
ANTXR1_13F	GAGCCTTAAATCTGCATATCA	2:69379205-69379225
ANTXR1_13R	TGGCAATCTCACACCCTAACT	2:69379587-69379607
ANTXR1_14F	AAACCAGAAGAGACGCAAATG	2:69397148-69397168
ANTXR1_14R	TGCTCTGCAGGGGGCTAAGTG	2:69397497-69397517
ANTXR1_1516F	AGTGATTGGCCCAAGGTTCTA	2:69408764-69408784
ANTXR1_1516R	TGATAAGCTGGGTTTTAGGTT	2:69409883-69409903
ANTXR1_17F	TGACTGAAGAAGCACGGAAAG	2:69420374-69420394

ANTXR1_17R	GCAACATGAAATAATAGCTGG	2:69420708-69420728
ANTXR1_18F	AGCACCCAGTTAAGGTCAGTC	2:69472088-69472108
ANTXR1_18R	TCATTTGTTTTCTGGCAATTT	2:69472793-69472813
Primers for RT-PCR Amplification of *ANTXR1*cDNA		
cANTXR1_1F	CCTGAGGGTCGTGGCGAGTTC	2:69240564-69240584
cANTXR1_1R	TAGGCGCTGGACACAGTAAAT	2:69350179-69350199
cANTXR1_ex1F	ATGGCCACGGCGGAGCGGAGA	2:69240632-69240652
cANTXR1_ex1R	AGGTCAAATCCGCCGTAGCAG	2:69240745-69240765
cANTXR1_ex3R	TTAAGGTTGTTCCTCGGGTGG	2:69271906-69271926
cANTXR1_ex56R	CGCTGGCTGTCCTGTACCCTT	2:69300152-69300171
cANTXR1_v3R	GAGGGAGCAGGCGGTATTCTC	2:69372511-69372531
cANTXR1_v2R	CGTTGCACGGGCTGTGTTAGG	2:69399556-69399576
cANTXR1_v1R	AGGTGTGGTAGGCGTTGTTGA	2:69472412-69472432
Primers for Quantitative PCR of *GAPDH* and *ANTXR1* cDNA		
GAPDH_c_F	GGATTTGGTCGTATTGGGCG	12:6645877-6645897
GAPDH_c_R	TCGCCCCACTTGATTTTGGA	12:6646096-6646115
cANTXR1_ex1F	ATGGCCACGGCGGAGCGGAGA	2:69240632-69240652
cANTXR1_ex3R	TTAAGGTTGTTCCTCGGGTGG	2:69271906-69271926
Primers for Quantitative PCR Analysis of the Genomic Fragment Spanning *ANTXR1* Mutations		
JUP_12R	GGAGACCCCCAAAAGTGTTGC	17:39913588-39913608
JUP_12F	GGCCCCACTCATGGAGTTGCT	17:39913909-39913929
ANTXR1_3F	TTCAGTTCTGGCAGCCGTGAT	2:69271766-69271786
ANTXR1_3R	ACCCATGTGCCCATACGTAAG	2:69272082-69272102
ANTXR1_11F	TTTCTGTCCTTGCGATAGTTT	2:69349983-69350003
ANTXR1_11R	GCTCCACTTTCTCTAGATGCT	2:69350294-69350314
ANTXR1_17F	TGACTGAAGAAGCACGGAAAG	2:69420374-69420394
ANTXR1_17R	GCAACATGAAATAATAGCTGG	2:69420708-69420728
FHL1_ex6U	GGCTCACCTTCTCCGAGCCTT	X:135290422-135290442
FHL1_ex6L	TGTATTGCAAAGGCTAACCTG	X:135290969-135290989

References

1. Littink, K.W., Koenekoop, R.K., van den Born, L.I., Collin, R.W., Moruz, L., Veltman, J.A., Roosing, S., Zonneveld, M.N., Omar, A., Darvish, M., et al. (2010). Homozygosity mapping in patients with cone-rod dystrophy: novel mutations and clinical characterizations. Invest Ophthalmol Vis Sci 51, 5943-5951.
2. Woods, C.G., Cox, J., Springell, K., Hampshire, D.J., Mohamed, M.D., McKibbin, M., Stern, R., Raymond, F.L., Sandford, R., Malik Sharif, S., et al. (2006). Quantification of homozygosity in consanguineous individuals with autosomal recessive disease. American journal of human genetics 78, 889-896.